Today's outline - November 04, 2024

Today's outline - November 04, 2024

- Dumond diagrams & monochromators

Today's outline - November 04, 2024

- Dumond diagrams & monochromators
- Photoelectric absorption

Today's outline - November 04, 2024

- Dumond diagrams & monochromators
- Photoelectric absorption
- X-ray absorption spectroscopy

Today's outline - November 04, 2024

- Dumond diagrams & monochromators
- Photoelectric absorption
- X-ray absorption spectroscopy
- EXAFS theory

Today's outline - November 04, 2024

- Dumond diagrams & monochromators
- Photoelectric absorption
- X-ray absorption spectroscopy
- EXAFS theory

Today's outline - November 04, 2024

- Dumond diagrams & monochromators
- Photoelectric absorption
- X-ray absorption spectroscopy
- EXAFS theory

Reading Assignment: Chapter 7.4

Today's outline - November 04, 2024

- Dumond diagrams & monochromators
- Photoelectric absorption
- X-ray absorption spectroscopy
- EXAFS theory

Reading Assignment: Chapter 7.4

Homework Assignment #06:
Chapter 6: 1,6,7,8,9
due Friday, November 15, 2024

Today's outline - November 04, 2024

- Dumond diagrams & monochromators
- Photoelectric absorption
- X-ray absorption spectroscopy
- EXAFS theory

Reading Assignment: Chapter 7.4

Homework Assignment #06:
Chapter 6: 1,6,7,8,9
due Friday, November 15, 2024

Homework Assignment #07:
Chapter 7: 2,3,9,10,11
due Monday, November 25, 2024

Beam line ID32 @ ESRF

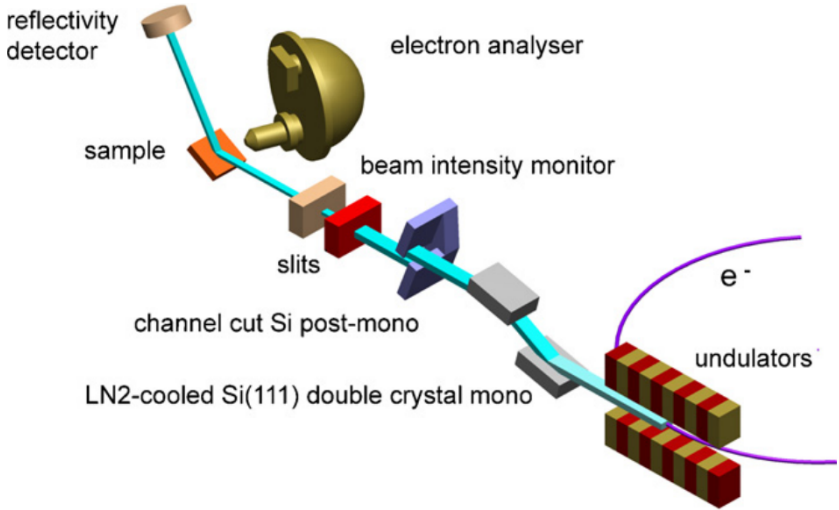

Structure of Sn on Ge(111)

The low temperature 3×3 structure (dashed line) is well known but the room temperature $\sqrt{3} \times \sqrt{3}$ surface structure (solid line) is unresolved

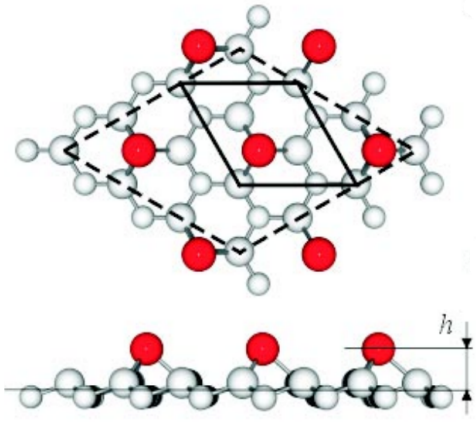

"Chemically resolved structure of the Sn/Ge(111) surface," T.-L. Lee, S. Warren, B.C.C. Cowie, and J. Zengenhagen, *Phys. Rev. Lett.* **96**, 046103 (2006).

Structure of Sn on Ge(111)

The low temperature 3×3 structure (dashed line) is well known but the room temperature $\sqrt{3} \times \sqrt{3}$ surface structure (solid line) is unresolved

A sub-monolayer of Sn is evaporated on a clean Ge(111) surface and studied using x-ray standing wave stimulated photoelectron spectroscopy

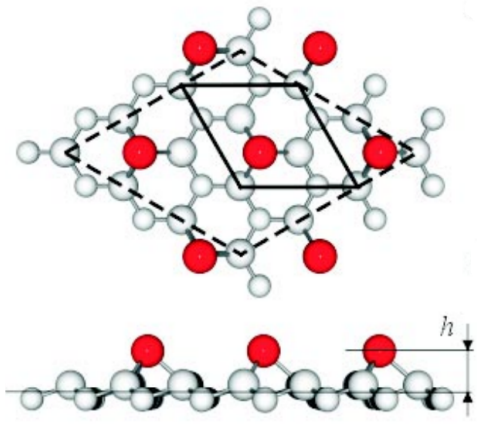

"Chemically resolved structure of the Sn/Ge(111) surface," T.-L. Lee, S. Warren, B.C.C. Cowie, and J. Zengenhagen, *Phys. Rev. Lett.* **96**, 046103 (2006).

Structure of Sn on Ge(111)

The low temperature 3×3 structure (dashed line) is well known but the room temperature $\sqrt{3} \times \sqrt{3}$ surface structure (solid line) is unresolved

A sub-monolayer of Sn is evaporated on a clean Ge(111) surface and studied using x-ray standing wave stimulated photoelectron spectroscopy

Below 0.2 ML, the well known 2×2 structure is measured as a reference

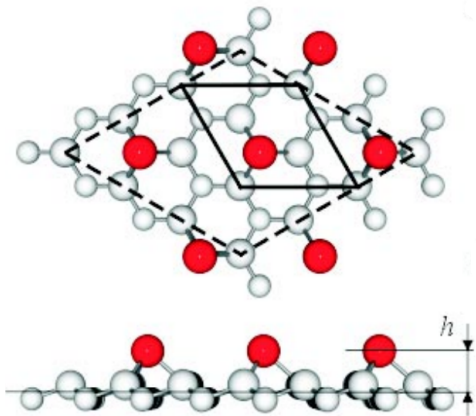

"Chemically resolved structure of the Sn/Ge(111) surface," T.-L. Lee, S. Warren, B.C.C. Cowie, and J. Zengenhagen, *Phys. Rev. Lett.* **96**, 046103 (2006).

Structure of Sn on Ge(111)

The low temperature 3×3 structure (dashed line) is well known but the room temperature $\sqrt{3} \times \sqrt{3}$ surface structure (solid line) is unresolved

A sub-monolayer of Sn is evaporated on a clean Ge(111) surface and studied using x-ray standing wave stimulated photoelectron spectroscopy

Below 0.2 ML, the well known 2×2 structure is measured as a reference

Above 0.2 ML, the $\sqrt{3} \times \sqrt{3}$ structure appears and then dominates

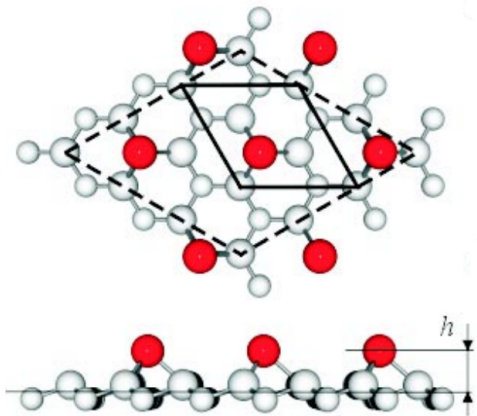

"Chemically resolved structure of the Sn/Ge(111) surface," T.-L. Lee, S. Warren, B.C.C. Cowie, and J. Zengenhagen, *Phys. Rev. Lett.* **96**, 046103 (2006).

Structure of Sn on Ge(111)

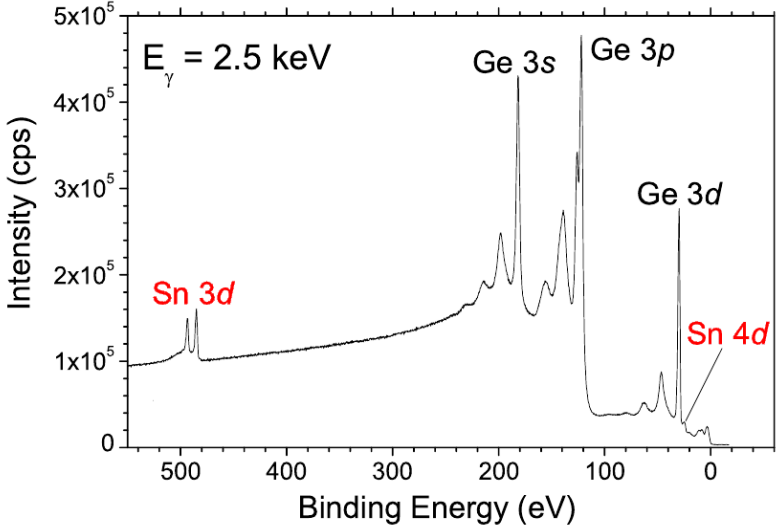

"Chemically resolved structure of the Sn/Ge(111) surface," T.-L. Lee, S. Warren, B.C.C. Cowie, and J. Zengenhagen, *Phys. Rev. Lett.* **96**, 046103 (2006).

Structure of Sn on Ge(111)

With an incident energy of 2.5 keV, the 2×2 and $\sqrt{3} \times \sqrt{3}$ structures are measured in an off-Bragg condition

"Chemically resolved structure of the Sn/Ge(111) surface," T.-L. Lee, S. Warren, B.C.C. Cowie, and J. Zengenhagen, *Phys. Rev. Lett.* **96**, 046103 (2006).

Structure of Sn on Ge(111)

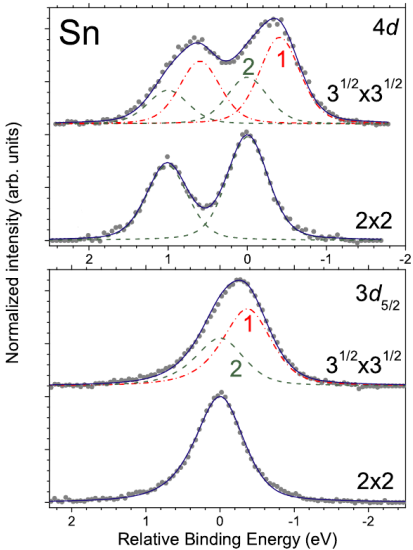

With an incident energy of 2.5 keV, the 2×2 and $\sqrt{3} \times \sqrt{3}$ structures are measured in an off-Bragg condition

The lines for both the Sn $3d_{5/2}$ and $4d$ peaks in the 2×2 phase are sharp, indicating a single chemical state

"Chemically resolved structure of the Sn/Ge(111) surface," T.-L. Lee, S. Warren, B.C.C. Cowie, and J. Zengenhagen, *Phys. Rev. Lett.* **96**, 046103 (2006).

Structure of Sn on Ge(111)

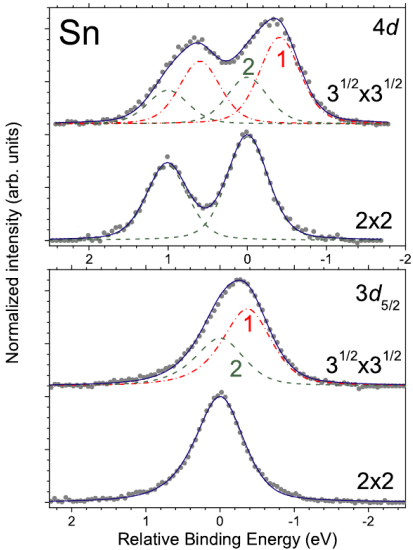

With an incident energy of 2.5 keV, the 2×2 and $\sqrt{3} \times \sqrt{3}$ structures are measured in an off-Bragg condition

The lines for both the Sn $3d_{5/2}$ and $4d$ peaks in the 2×2 phase are sharp, indicating a single chemical state

The $\sqrt{3} \times \sqrt{3}$ structure shows two distinct chemical shifts, with the majority component, I_1, having a slightly lower binding energy than the minority component, I_2

"Chemically resolved structure of the Sn/Ge(111) surface," T.-L. Lee, S. Warren, B.C.C. Cowie, and J. Zengenhagen, *Phys. Rev. Lett.* **96**, 046103 (2006).

Structure of Sn on Ge(111)

By varying the energy with a resolution of 500 meV, the standing wave is swept through the Sn layer

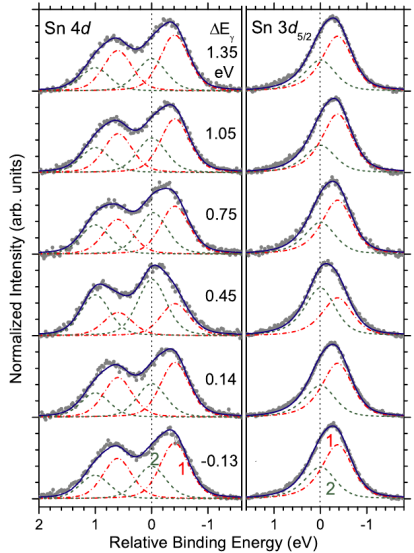

"Chemically resolved structure of the Sn/Ge(111) surface," T.-L. Lee, S. Warren, B.C.C. Cowie, and J. Zengenhagen, *Phys. Rev. Lett.* **96**, 046103 (2006).

Structure of Sn on Ge(111)

By varying the energy with a resolution of 500 meV, the standing wave is swept through the Sn layer

As the energy is scanned around the center of the Ge(111) reflection, the fits using a mixture of Gaussian and Lorentzian line shapes show that the relative intensity, I_1/I_2 varies

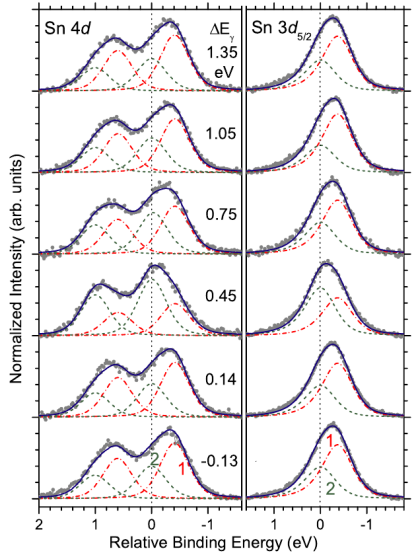

"Chemically resolved structure of the Sn/Ge(111) surface," T.-L. Lee, S. Warren, B.C.C. Cowie, and J. Zengenhagen, *Phys. Rev. Lett.* **96**, 046103 (2006).

Structure of Sn on Ge(111)

By varying the energy with a resolution of 500 meV, the standing wave is swept through the Sn layer

As the energy is scanned around the center of the Ge(111) reflection, the fits using a mixture of Gaussian and Lorentzian line shapes show that the relative intensity, I_1/I_2 varies

At $\Delta E_\gamma = 0.45$ eV, the I_1/I_2 ratio almost completely inverts, showing that the two atom populations are at different heights above the surface

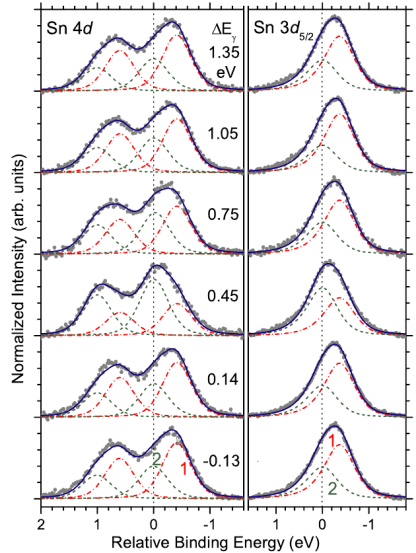

"Chemically resolved structure of the Sn/Ge(111) surface," T.-L. Lee, S. Warren, B.C.C. Cowie, and J. Zengenhagen, *Phys. Rev. Lett.* **96**, 046103 (2006).

Structure of Sn on Ge(111)

The normalized peak intensities can be fitted to extract the relative positions of the two populations of atoms and their atomic ratio

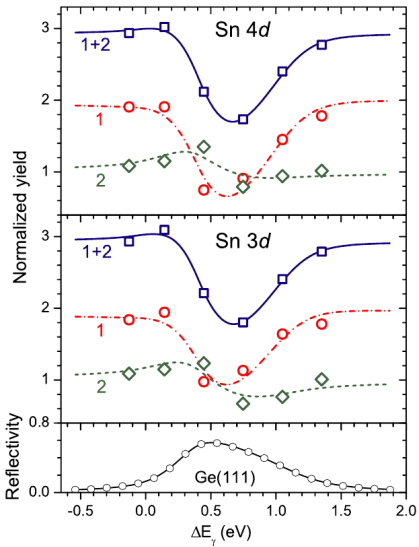

"Chemically resolved structure of the Sn/Ge(111) surface," T.-L. Lee, S. Warren, B.C.C. Cowie, and J. Zengenhagen, *Phys. Rev. Lett.* **96**, 046103 (2006).

Structure of Sn on Ge(111)

The normalized peak intensities can be fitted to extract the relative positions of the two populations of atoms and their atomic ratio

Population 1 is two times larger than population 2 and is located a height $\Delta h = 0.23$ Å further from the Ge(111) surface

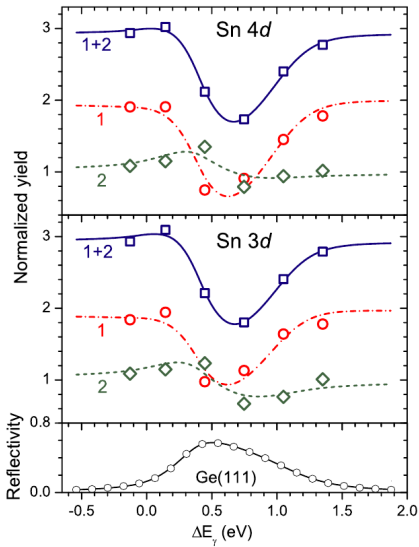

"Chemically resolved structure of the Sn/Ge(111) surface," T.-L. Lee, S. Warren, B.C.C. Cowie, and J. Zengenhagen, *Phys. Rev. Lett.* **96**, 046103 (2006).

Structure of Sn on Ge(111)

The normalized peak intensities can be fitted to extract the relative positions of the two populations of atoms and their atomic ratio

Population 1 is two times larger than population 2 and is located a height $\Delta h = 0.23$ Å further from the Ge(111) surface

Population 1 also has a lower binding energy, demonstrating that the binding energy is directly correlated to the height from the surface

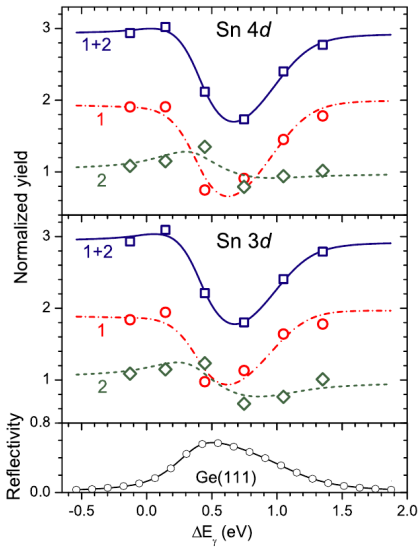

"Chemically resolved structure of the Sn/Ge(111) surface," T.-L. Lee, S. Warren, B.C.C. Cowie, and J. Zengenhagen, *Phys. Rev. Lett.* **96**, 046103 (2006).

Asymmetric geometry

When the diffracting planes are not precisely aligned with the surface of the crystal the asymmetry angle, α, is the important parameter

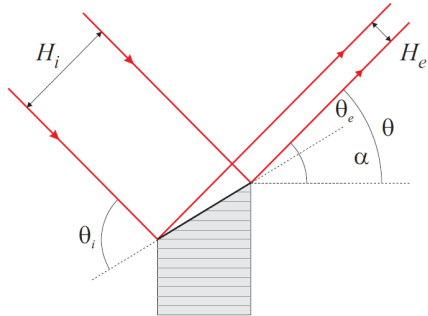

Asymmetric geometry

When the diffracting planes are not precisely aligned with the surface of the crystal the asymmetry angle, α, is the important parameter

$$0 < \alpha < \theta_{Bragg}$$

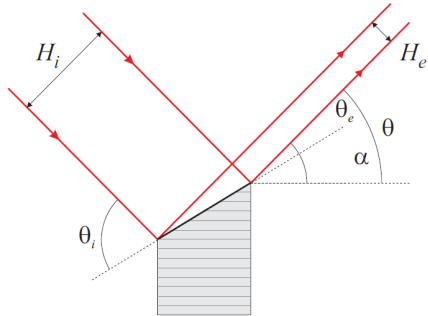

Asymmetric geometry

When the diffracting planes are not precisely aligned with the surface of the crystal the asymmetry angle, α, is the important parameter

$$0 < \alpha < \theta_{Bragg}$$

this leads to a beam compression

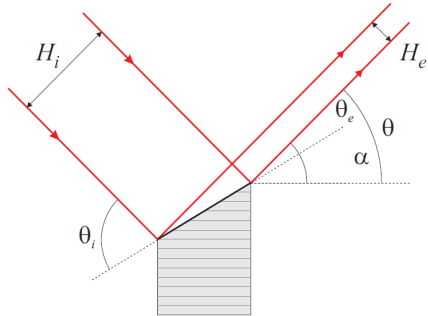

Asymmetric geometry

When the diffracting planes are not precisely aligned with the surface of the crystal the asymmetry angle, α, is the important parameter

$$0 < \alpha < \theta_{Bragg}$$

this leads to a beam compression

$$b = \frac{\sin\theta_i}{\sin\theta_e}$$

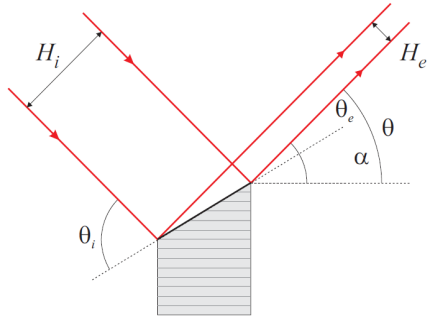

Asymmetric geometry

When the diffracting planes are not precisely aligned with the surface of the crystal the asymmetry angle, α, is the important parameter

$$0 < \alpha < \theta_{Bragg}$$

this leads to a beam compression

$$b = \frac{\sin\theta_i}{\sin\theta_e} = \frac{\sin(\theta+\alpha)}{\sin(\theta-\alpha)}$$

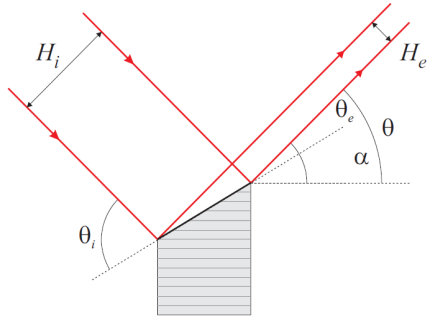

Asymmetric geometry

When the diffracting planes are not precisely aligned with the surface of the crystal the asymmetry angle, α, is the important parameter

$$0 < \alpha < \theta_{Bragg}$$

this leads to a beam compression

$$b = \frac{\sin\theta_i}{\sin\theta_e} = \frac{\sin(\theta+\alpha)}{\sin(\theta-\alpha)} \quad \longrightarrow \quad H_e = \frac{H_i}{b}$$

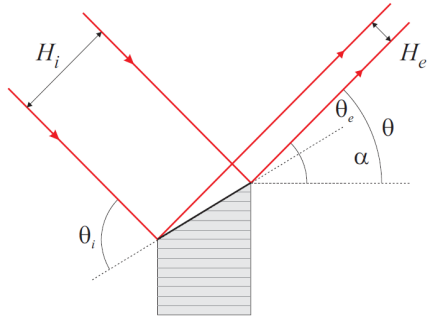

Asymmetric geometry

When the diffracting planes are not precisely aligned with the surface of the crystal the asymmetry angle, α, is the important parameter

$$0 < \alpha < \theta_{Bragg}$$

this leads to a beam compression

$$b = \frac{\sin\theta_i}{\sin\theta_e} = \frac{\sin(\theta+\alpha)}{\sin(\theta-\alpha)} \quad \longrightarrow \quad H_e = \frac{H_i}{b}$$

according to Liouville's theorem, phase space is invariant so the divergence of the beam, $\delta\theta$, must also change

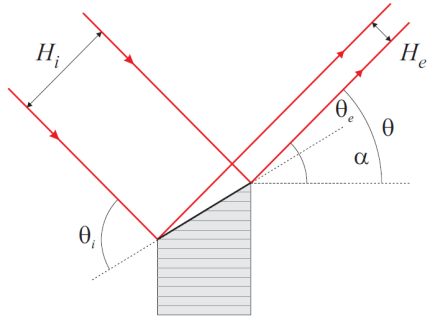

Asymmetric geometry

When the diffracting planes are not precisely aligned with the surface of the crystal the asymmetry angle, α, is the important parameter

$$0 < \alpha < \theta_{Bragg}$$

this leads to a beam compression

$$b = \frac{\sin\theta_i}{\sin\theta_e} = \frac{\sin(\theta+\alpha)}{\sin(\theta-\alpha)} \quad \longrightarrow \quad H_e = \frac{H_i}{b}$$

according to Liouville's theorem, phase space is invariant so the divergence of the beam, $\delta\theta$, must also change

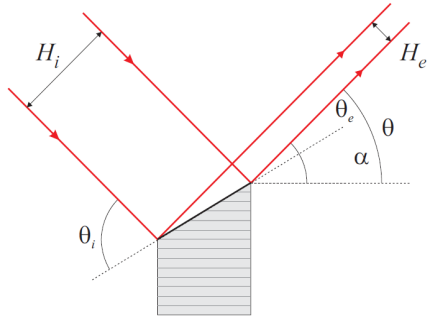

$$\delta\theta_e = \sqrt{b}(\zeta_D \tan\theta)$$

Asymmetric geometry

When the diffracting planes are not precisely aligned with the surface of the crystal the asymmetry angle, α, is the important parameter

$$0 < \alpha < \theta_{Bragg}$$

this leads to a beam compression

$$b = \frac{\sin\theta_i}{\sin\theta_e} = \frac{\sin(\theta+\alpha)}{\sin(\theta-\alpha)} \quad \longrightarrow \quad H_e = \frac{H_i}{b}$$

according to Liouville's theorem, phase space is invariant so the divergence of the beam, $\delta\theta$, must also change

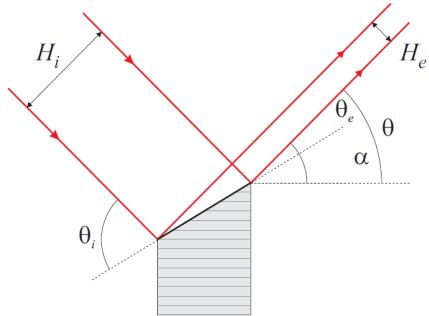

$$\delta\theta_e = \sqrt{b}(\zeta_D \tan\theta)$$

$$\delta\theta_i = \frac{1}{\sqrt{b}}(\zeta_D \tan\theta)$$

Asymmetric geometry

When the diffracting planes are not precisely aligned with the surface of the crystal the asymmetry angle, α, is the important parameter

$$0 < \alpha < \theta_{Bragg}$$

this leads to a beam compression

$$b = \frac{\sin\theta_i}{\sin\theta_e} = \frac{\sin(\theta+\alpha)}{\sin(\theta-\alpha)} \quad \longrightarrow \quad H_e = \frac{H_i}{b}$$

according to Liouville's theorem, phase space is invariant so the divergence of the beam, $\delta\theta$, must also change

$$\delta\theta_i H_i$$

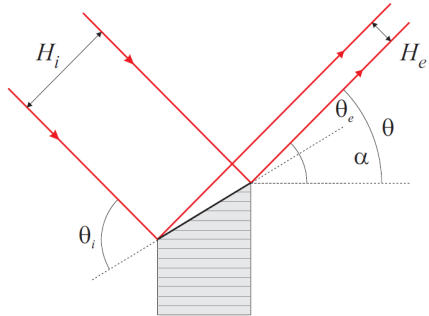

$$\delta\theta_e = \sqrt{b}(\zeta_D \tan\theta)$$

$$\delta\theta_i = \frac{1}{\sqrt{b}}(\zeta_D \tan\theta)$$

Asymmetric geometry

When the diffracting planes are not precisely aligned with the surface of the crystal the asymmetry angle, α, is the important parameter

$$0 < \alpha < \theta_{Bragg}$$

this leads to a beam compression

$$b = \frac{\sin\theta_i}{\sin\theta_e} = \frac{\sin(\theta+\alpha)}{\sin(\theta-\alpha)} \quad \longrightarrow \quad H_e = \frac{H_i}{b}$$

according to Liouville's theorem, phase space is invariant so the divergence of the beam, $\delta\theta$, must also change

$$\delta\theta_i H_i = \frac{1}{\sqrt{b}}(\zeta_D \tan\theta) b H_e$$

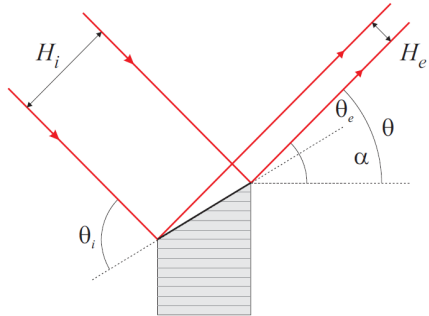

$$\delta\theta_e = \sqrt{b}(\zeta_D \tan\theta)$$

$$\delta\theta_i = \frac{1}{\sqrt{b}}(\zeta_D \tan\theta)$$

Asymmetric geometry

When the diffracting planes are not precisely aligned with the surface of the crystal the asymmetry angle, α, is the important parameter

$$0 < \alpha < \theta_{Bragg}$$

this leads to a beam compression

$$b = \frac{\sin\theta_i}{\sin\theta_e} = \frac{\sin(\theta+\alpha)}{\sin(\theta-\alpha)} \quad \longrightarrow \quad H_e = \frac{H_i}{b}$$

according to Liouville's theorem, phase space is invariant so the divergence of the beam, $\delta\theta$, must also change

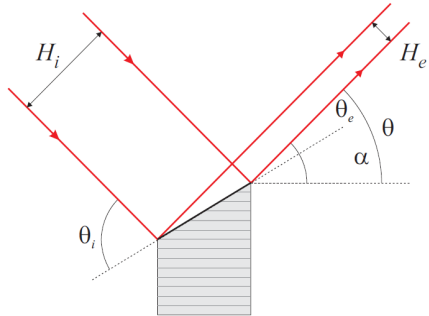

$$\delta\theta_e = \sqrt{b}(\zeta_D \tan\theta)$$

$$\delta\theta_i = \frac{1}{\sqrt{b}}(\zeta_D \tan\theta)$$

$$\delta\theta_i H_i = \frac{1}{\sqrt{b}}(\zeta_D \tan\theta) b H_e = \sqrt{b}(\zeta_D \tan\theta) H_e$$

Asymmetric geometry

When the diffracting planes are not precisely aligned with the surface of the crystal the asymmetry angle, α, is the important parameter

$$0 < \alpha < \theta_{Bragg}$$

this leads to a beam compression

$$b = \frac{\sin\theta_i}{\sin\theta_e} = \frac{\sin(\theta+\alpha)}{\sin(\theta-\alpha)} \quad \longrightarrow \quad H_e = \frac{H_i}{b}$$

according to Liouville's theorem, phase space is invariant so the divergence of the beam, $\delta\theta$, must also change

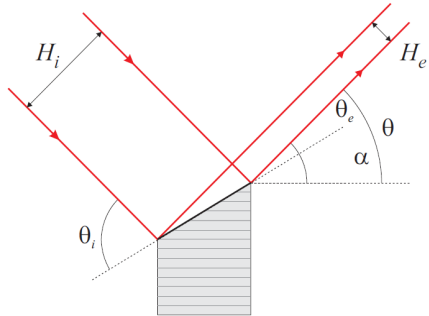

$$\delta\theta_e = \sqrt{b}(\zeta_D \tan\theta)$$

$$\delta\theta_i = \frac{1}{\sqrt{b}}(\zeta_D \tan\theta)$$

$$\delta\theta_i H_i = \frac{1}{\sqrt{b}}(\zeta_D \tan\theta) b H_e = \sqrt{b}(\zeta_D \tan\theta) H_e = \delta\theta_e H_e$$

Rocking curve measurements

The measured "rocking" curve from a two crystal system is a convolution of the Darwin curves of both crystals.

Rocking curve measurements

The measured "rocking" curve from a two crystal system is a convolution of the Darwin curves of both crystals. When the two crystals have a matched asymmetry, we get a triangle.

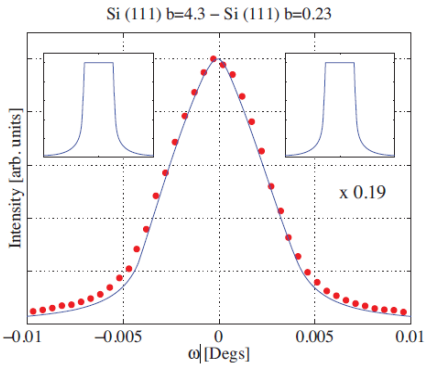

output divergence on left, input divergence on right

Rocking curve measurements

The measured "rocking" curve from a two crystal system is a convolution of the Darwin curves of both crystals. When the two crystals have a matched asymmetry, we get a triangle.

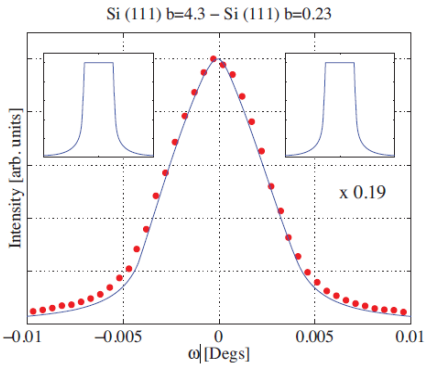

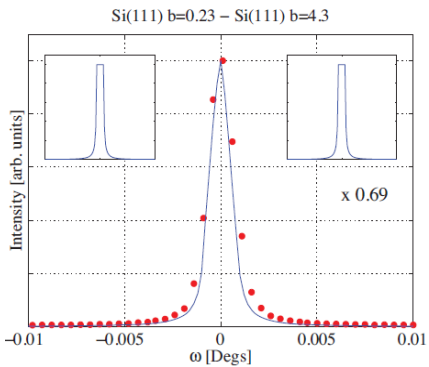

output divergence on left, input divergence on right

Rocking curve measurements

The measured "rocking" curve from a two crystal system is a convolution of the Darwin curves of both crystals. When the two crystals have a matched asymmetry, we get a triangle. When one asymmetry is much higher, then we can measure the Darwin curve of a single crystal.

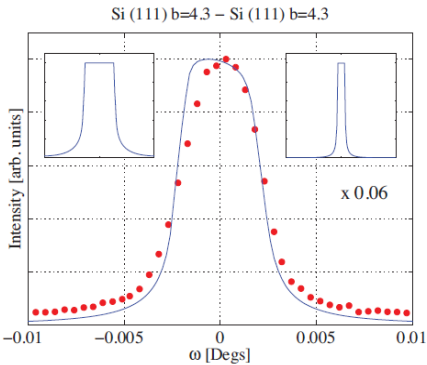

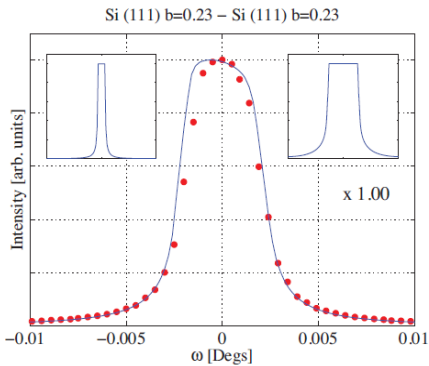

output divergence on left, input divergence on right

Dumond diagram: no Darwin width

Transfer function of an optical element parametrized by angle and wavelength.

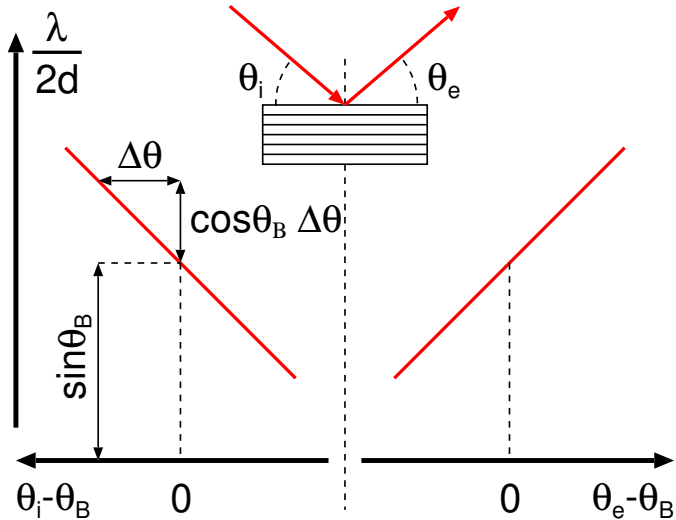

Dumond diagram: no Darwin width

Transfer function of an optical element parametrized by angle and wavelength. Here Darwin width is ignored.

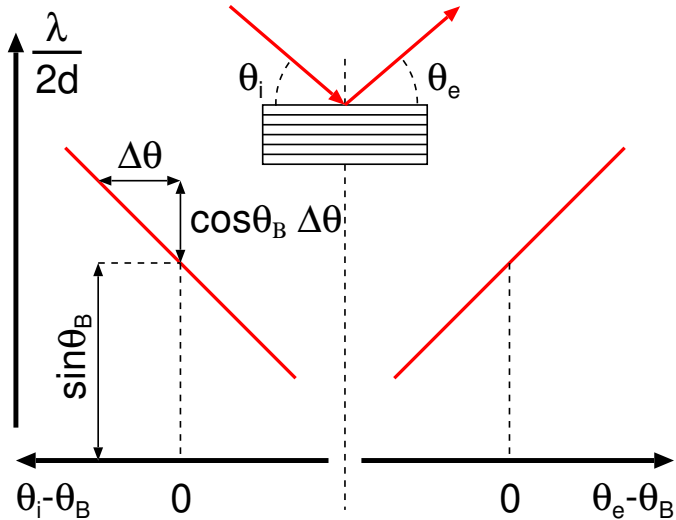

Dumond diagram: no Darwin width

Transfer function of an optical element parametrized by angle and wavelength. Here Darwin width is ignored.

for small angular deviations $\sin\theta$ is linear with a slope of $\cos\theta_B$

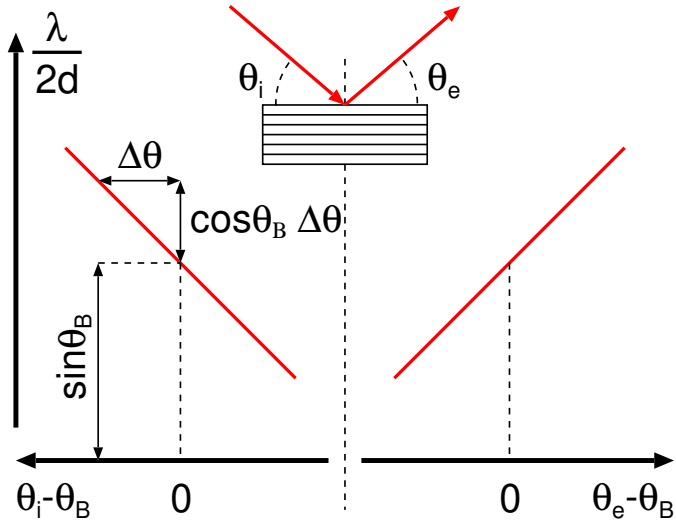

Dumond diagram: no Darwin width

Transfer function of an optical element parametrized by angle and wavelength. Here Darwin width is ignored.

for small angular deviations $\sin\theta$ is linear with a slope of $\cos\theta_B$

non-zero diffracted beam only for points on the line

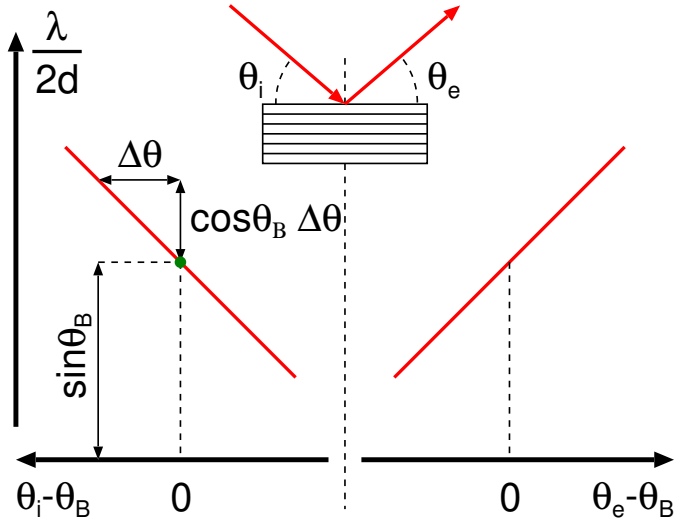

Dumond diagram: no Darwin width

Transfer function of an optical element parametrized by angle and wavelength. Here Darwin width is ignored.

for small angular deviations $\sin\theta$ is linear with a slope of $\cos\theta_B$

non-zero diffracted beam only for points on the line

a horizontal line transfers input to output beam characteristics

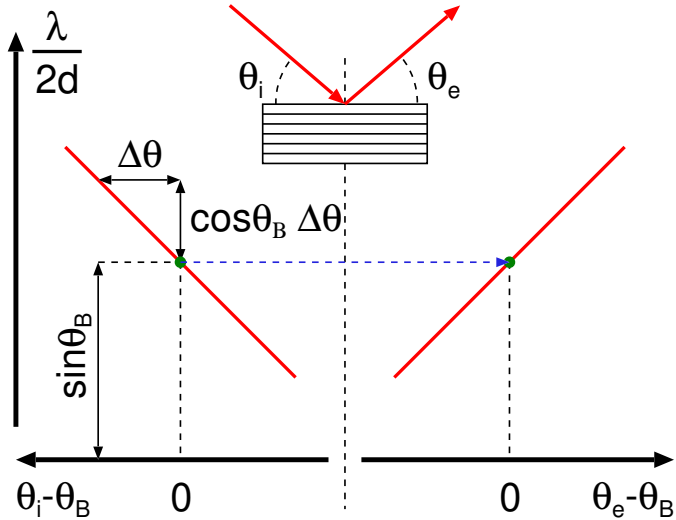

Dumond diagram: symmetric Bragg

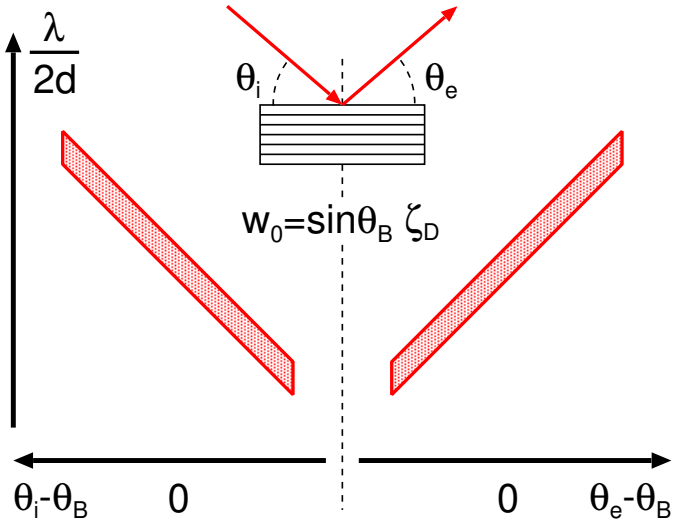

If Darwin width is included, the Bragg condition is represented by a box

Dumond diagram: symmetric Bragg

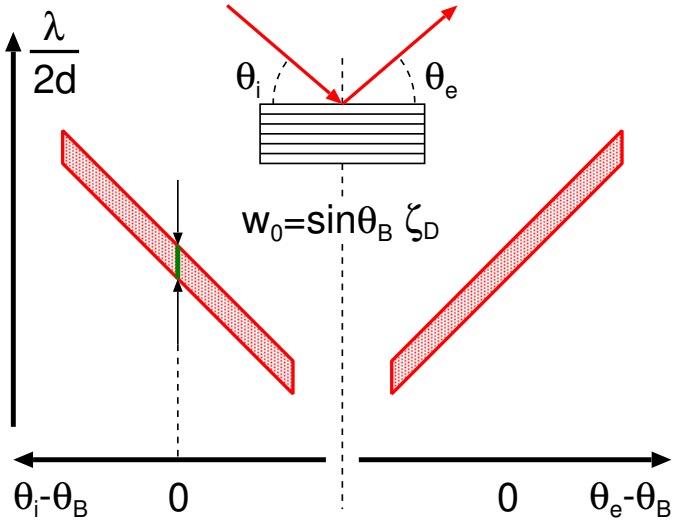

If Darwin width is included, the Bragg condition is represented by a box

for a perfectly collimated (no angular divergence) input beam, a bandwidth of radiation is accepted by the crystal

Dumond diagram: symmetric Bragg

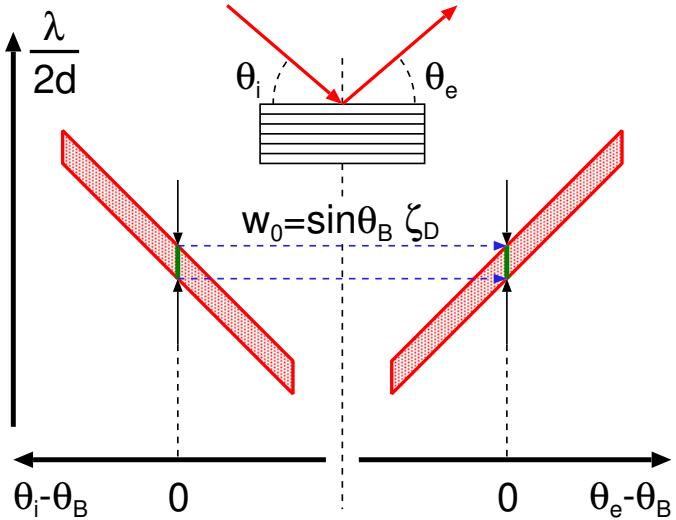

If Darwin width is included, the Bragg condition is represented by a box

for a perfectly collimated (no angular divergence) input beam, a bandwidth of radiation is accepted by the crystal

this input bandwidth is transferred to a similar output bandwidth which is also collimated

Dumond diagram: asymmetric Bragg

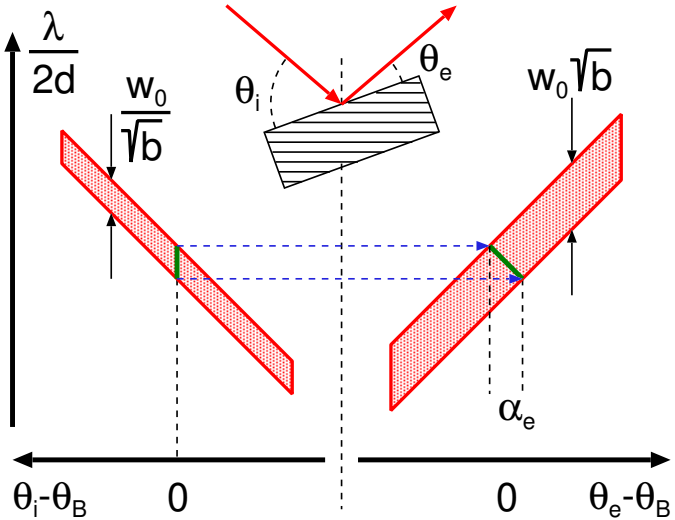

For an asymmetric crystal, the output beam is no longer collimated but acquires a divergence α_e

Dumond diagram: asymmetric Bragg

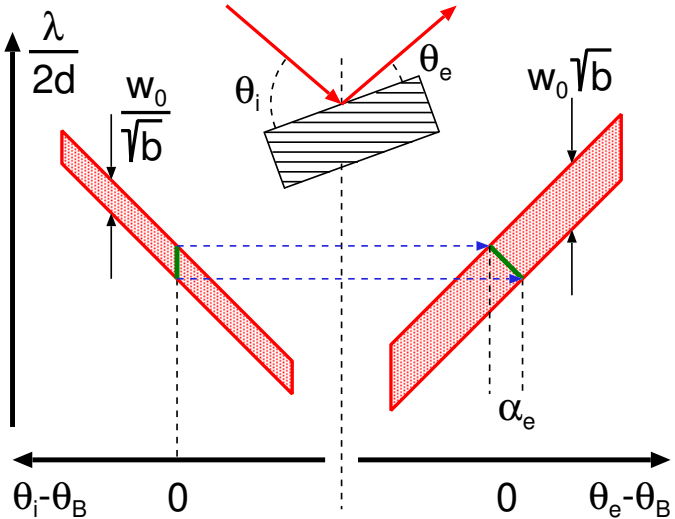

For an asymmetric crystal, the output beam is no longer collimated but acquires a divergence α_e

a perfectly collimated input beam transfers to an output beam that has an angular divergence which depends on the asymmetry factor *b*

Dumond diagram: asymmetric Bragg

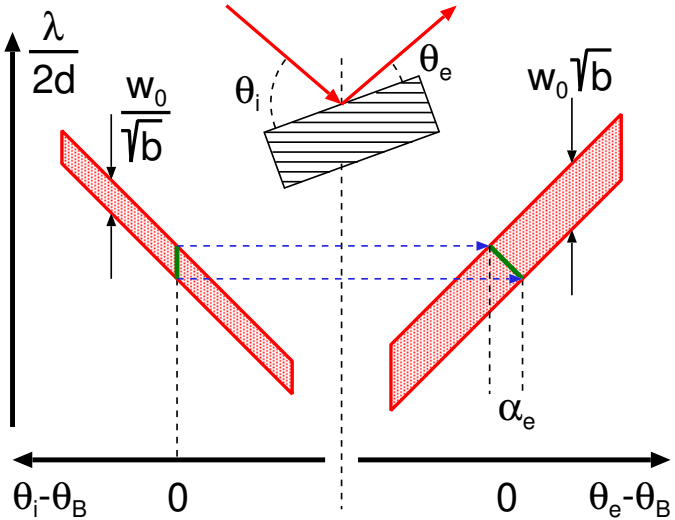

For an asymmetric crystal, the output beam is no longer collimated but acquires a divergence α_e

a perfectly collimated input beam transfers to an output beam that has an angular divergence which depends on the asymmetry factor *b*

this is in addition to a compression (in this case) of the beam height (Liouville's theorem!)

Double crystal monochromator: Non-dispersive

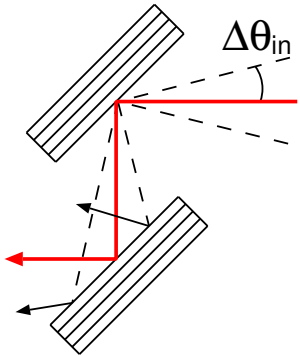

Double crystal monochromator: Non-dispersive

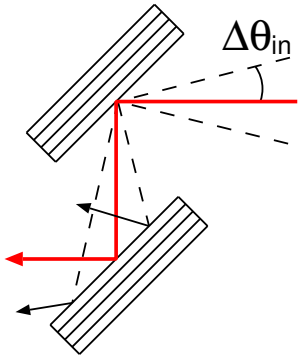

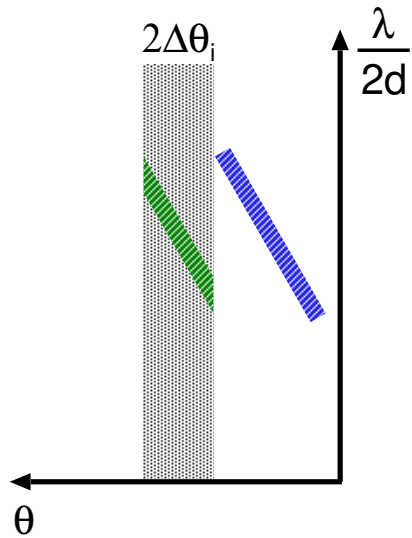

Double crystal monochromator: Non-dispersive

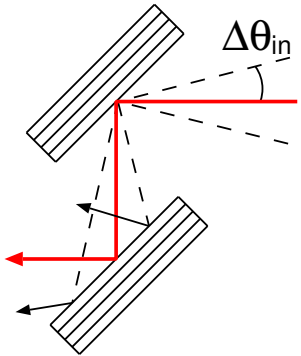

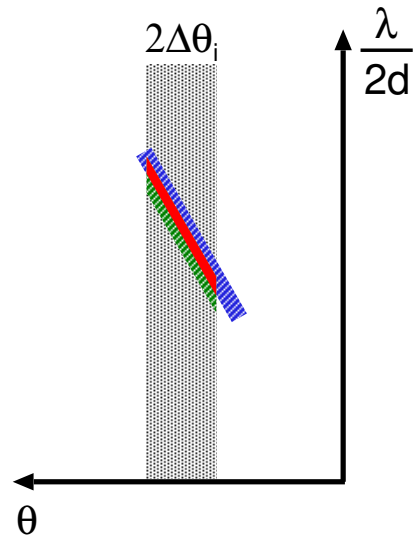

Double crystal monochromator: Non-dispersive

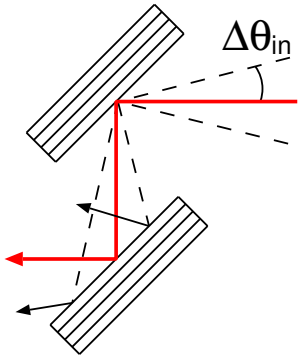

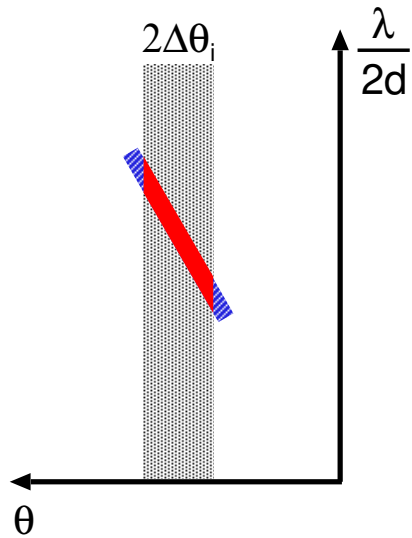

Double crystal monochromator: Non-dispersive

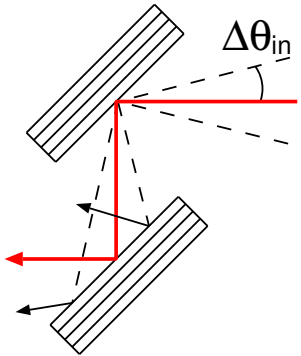

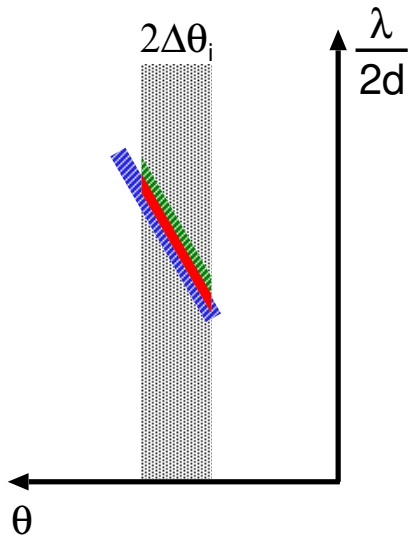

Double crystal monochromator: Non-dispersive

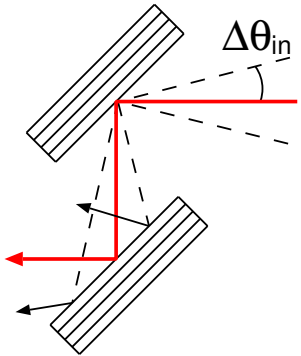

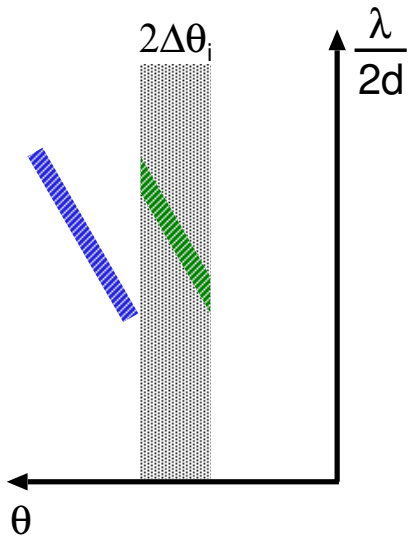

the transfer functions of the two crystals match and full bandwith and divergence is preserved, giving a triangle intensity curve

Double crystal monochromators: Dispersive

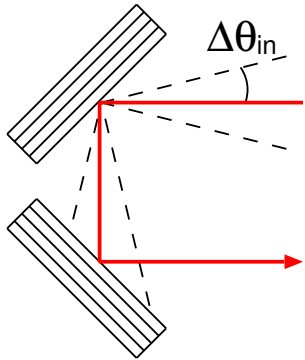

Double crystal monochromators: Dispersive

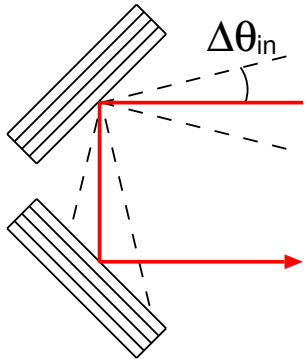

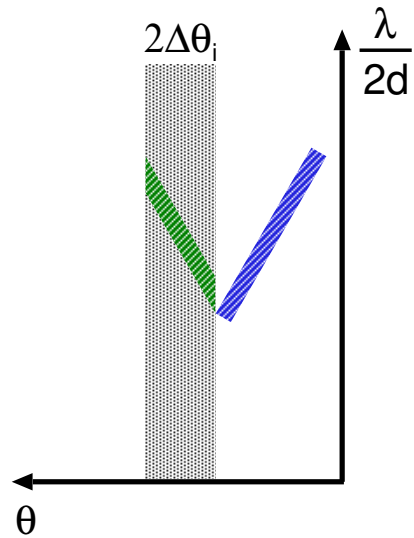

Double crystal monochromators: Dispersive

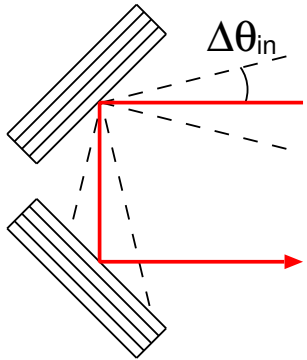

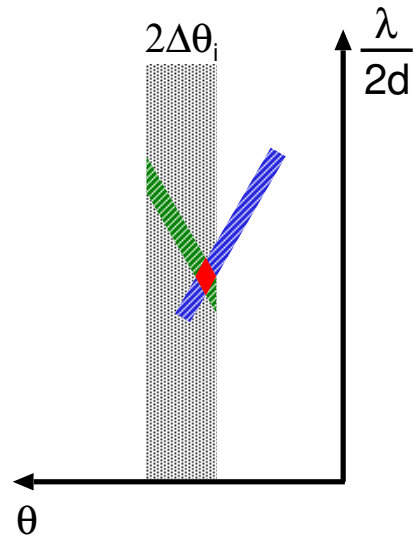

Double crystal monochromators: Dispersive

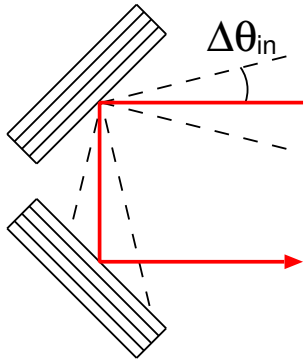

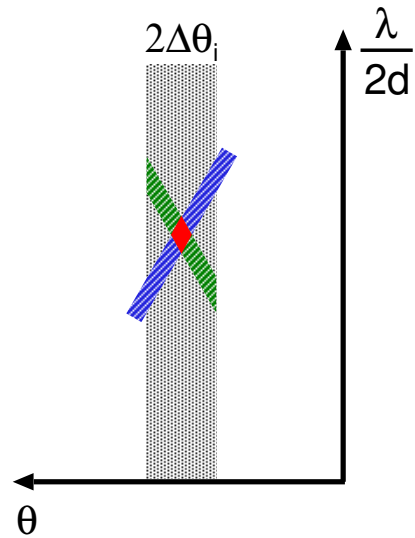

Double crystal monochromators: Dispersive

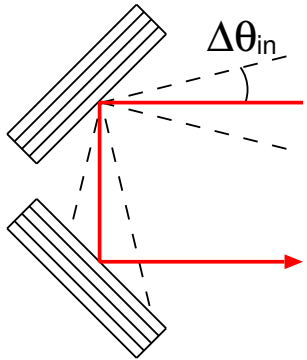

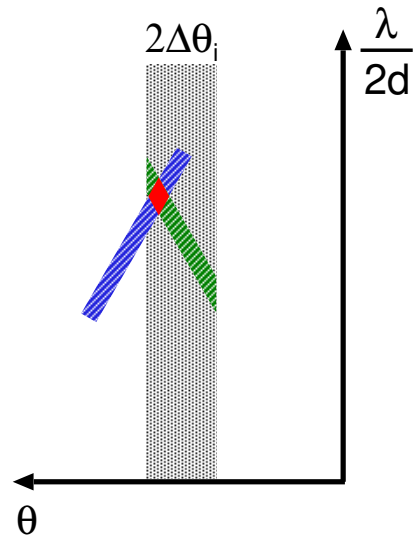

Double crystal monochromators: Dispersive

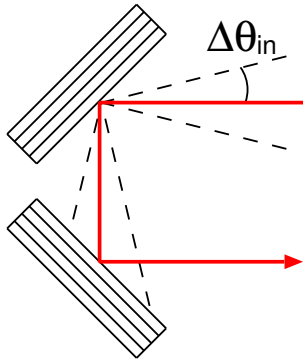

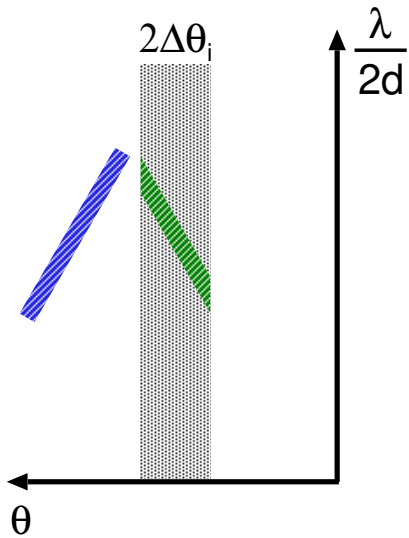

the transfer function matches only in a small energy band that varies with angle of the second crystal, mapping out the Darwin curve of the first crystal

Asymmetric monochromator at ELETTRA

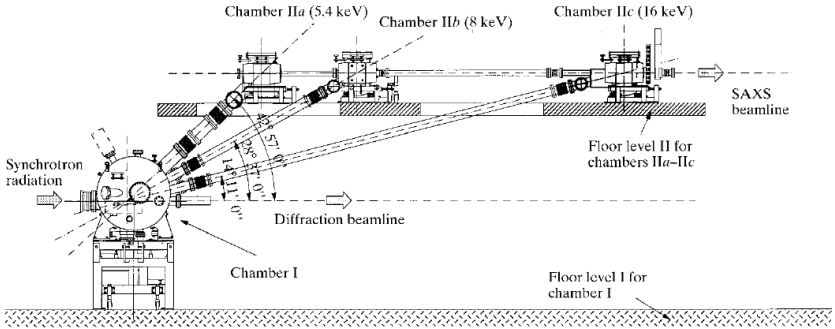

"High-throughput asymmetric double-crystal monochromator of the SAXS beamline at ELETTRA," S. Bernstorff, H. Amentisch, and P. Laggner, *J. Synchrotron Rad.* **5**, 1215-1221 (1998).

Asymmetric monochromator at ELETTRA

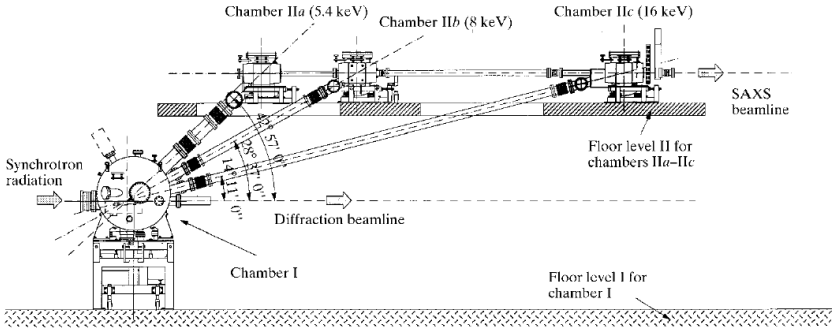

The SAXS beamline at ELETTRA has asymmetric cut crystals with 2° grazing incidence in order to spread the heat load

"High-throughput asymmetric double-crystal monochromator of the SAXS beamline at ELETTRA," S. Bernstorff, H. Amentisch, and P. Laggner, *J. Synchrotron Rad.* **5**, 1215-1221 (1998).

Asymmetric monochromator at ELETTRA

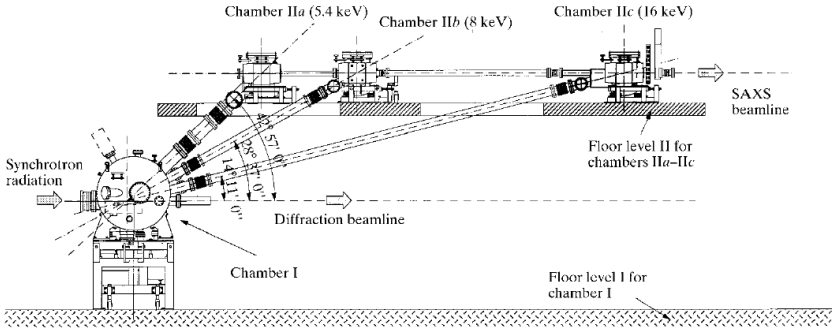

The SAXS beamline at ELETTRA has asymmetric cut crystals with 2° grazing incidence in order to spread the heat load

The three crystals are set for single energies of 5.6, 8.0, and 16 keV with a vertical displacement of 1.5 m and asymmetry parameter, b, of 0.053, 0.078, and 0.17, respectively

"High-throughput asymmetric double-crystal monochromator of the SAXS beamline at ELETTRA," S. Bernstorff, H. Amentisch, and P. Laggner, *J. Synchrotron Rad.* **5**, 1215-1221 (1998).

Total cross section

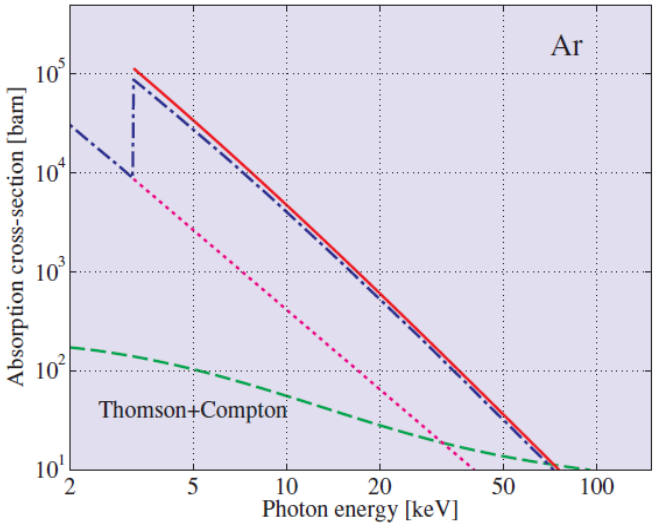

The total cross-section for photon "absorption" includes elastic (or coherent) scattering, Compton (inelastic) scattering, and photoelectric absorption.

Total cross section

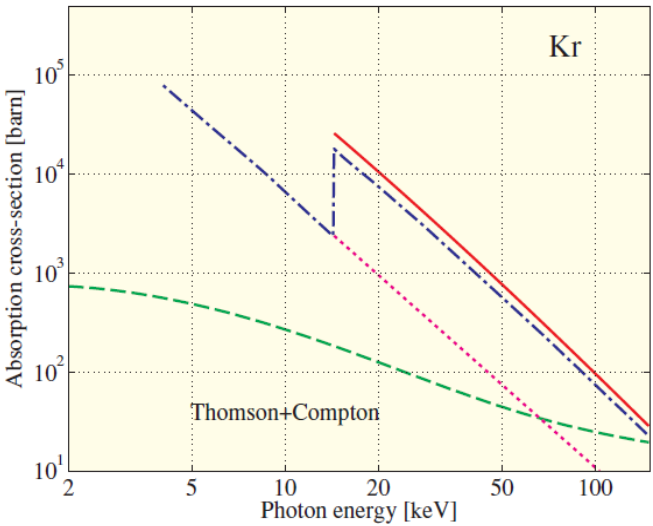

The total cross-section for photon "absorption" includes elastic (or coherent) scattering, Compton (inelastic) scattering, and photoelectric absorption.

Characteristic absorption jumps depend on the element

Total cross section

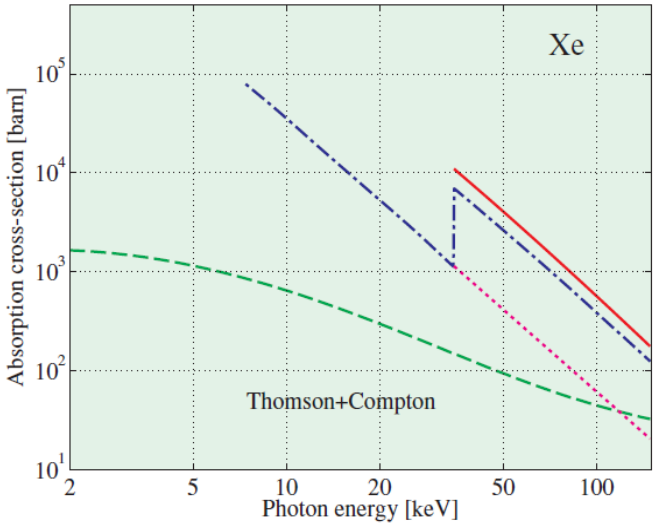

The total cross-section for photon "absorption" includes elastic (or coherent) scattering, Compton (inelastic) scattering, and photoelectric absorption.

Characteristic absorption jumps depend on the element

These quantities vary significantly over many decades but can easily put on an equal footing.

Scaled absorption

$$T = \frac{I}{I_0} = e^{-\mu z}$$

Scaled absorption

$$T = \frac{I}{I_0} = e^{-\mu z}$$

$$\mu = \frac{\rho_m N_A}{M} \sigma_a$$

Scaled absorption

$$T = \frac{I}{I_0} = e^{-\mu z}$$

$$\mu = \frac{\rho_m N_A}{M} \sigma_a$$

$$\sigma_a \sim \frac{Z^4}{E^3}$$

Scaled absorption

$$T = \frac{I}{I_0} = e^{-\mu z}$$
$$\mu = \frac{\rho_m N_A}{M}\sigma_a$$
$$\sigma_a \sim \frac{Z^4}{E^3}$$

σ_a can be scaled for different elements by E^3/Z^4 and plotted together

Scaled absorption

$$T = \frac{I}{I_0} = e^{-\mu z}$$

$$\mu = \frac{\rho_m N_A}{M}\sigma_a$$

$$\sigma_a \sim \frac{Z^4}{E^3}$$

σ_a can be scaled for different elements by E^3/Z^4 and plotted together

remarkably, all values lie on a common curve above the K edge and between the L and K edges and below the L edge

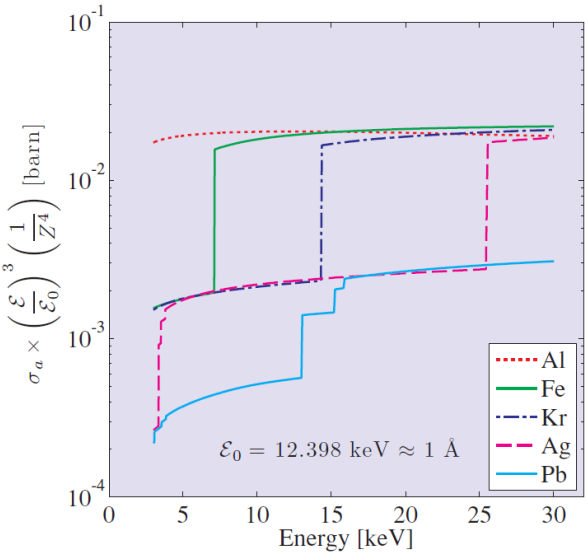

Absorption edge nomenclature

The states are labeled according to the principal, orbital angular momentum, and total angular momentum quantum numbers, n, l, and j, respectively

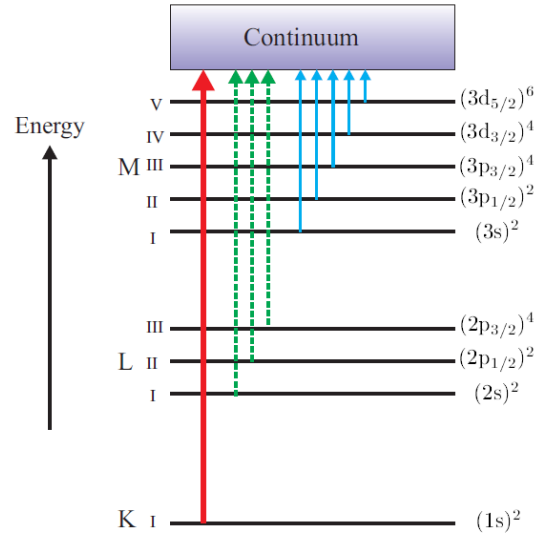

Absorption edge nomenclature

The states are labeled according to the principal, orbital angular momentum, and total angular momentum quantum numbers, n, l, and j, respectively

The absorption edges are labeled according to the initial principal quantum number of the photoelectron:

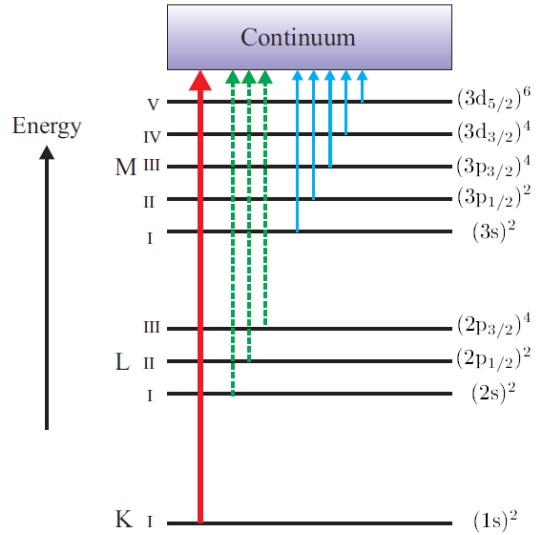

Absorption edge nomenclature

The states are labeled according to the principal, orbital angular momentum, and total angular momentum quantum numbers, n, l, and j, respectively

The absorption edges are labeled according to the initial principal quantum number of the photoelectron:

$$n = 1 \longrightarrow K$$
$$n = 2 \longrightarrow L$$
$$n = 3 \longrightarrow M$$

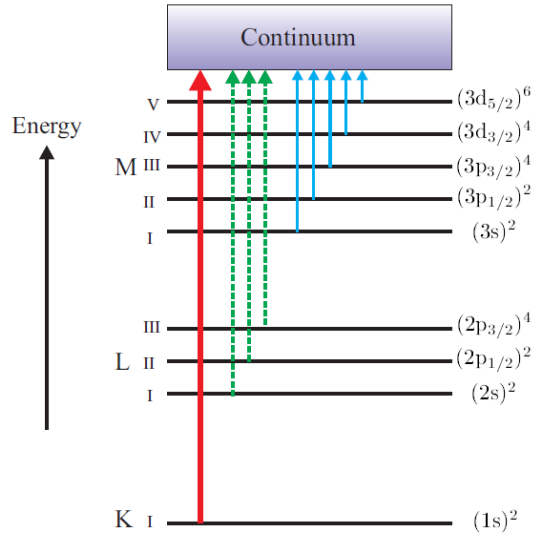

Absorption edge nomenclature

The states are labeled according to the principal, orbital angular momentum, and total angular momentum quantum numbers, n, l, and j, respectively

The absorption edges are labeled according to the initial principal quantum number of the photoelectron:

$$n = 1 \longrightarrow K$$
$$n = 2 \longrightarrow L$$
$$n = 3 \longrightarrow M$$

Roman numerals increase from low to high values of l and j